PROCEEDINGS of the
23rd International Congress on Acoustics
9 to 13 September 2019 in Aachen, Germany

Derivation of time-domain surface impedance boundary conditions based on in-situ surface measurements and model fitting

Baltazar BRIERE DE LA HOSSERAYE[1], Huiqing WANG[1], Fotis GEORGIOU[1], Maarten HORNIKX[1], Philip W. ROBINSON[2]

[1]Eindhoven University of Technology, The Netherlands, b.g.j.briere.de.la.hosseraye@tue.nl
[5]Facebook & Oculus, The United States, philrob22@fb.com

Abstract

In order to achieve accurate time-domain wave-based simulations of a real room, the acoustical properties of the locally reacting materials within the room have to be implemented as time-domain impedance boundary conditions (TDIBC), in such a way that the behavior of the materials is well-simulated within the wave-based solver. This paper presents the implementation of such TDIBCs of two materials: a porous absorber and an acoustic carpet. Firstly, the material properties were measured both in the impedance tube and in-situ with a pressure-velocity sensor. Advantages and drawbacks experienced with both methods in this context will be presented. Next, the measurement results were fitted to broadband impedance models to extend impedance data to the lower frequency range (20 Hz – 300 Hz), resulting in broadband impedance data (20 Hz - 4000 Hz). Finally the TDIBCs, in the form of complex reflection coefficients, were fitted as discrete sums of rational functions.

Keywords: Time-domain boundary condition; In situ measurement

1 INTRODUCTION

The accurate modelling of the acoustical properties of surfaces used as BCs is one of the challenges inherent to room acoustics simulations, as the accuracy of the results will depend on the proper modelling of the BCs, regardless of the algorithm used. The required boundary conditions data differs depending on the simulation method. For geometrical acoustics algorithms, the random incidence absorption coefficient is normally used. For wave-based methods in the time-domain, which is of interest in this paper, data of the surface impedance (or reflection coefficient) is needed. Moreover, if the surface impedance is obtained in the frequency domain, as it usually results from measurements, it is required to translate it into time-domain boundary conditions (TDBCs).

This paper proposes a three-steps methodology to implement such TDBCs from measurement data, for the Discontinuous Galerkin (DG) simulation of a reverberant room treated with two materials that can be treated as locally reacting: a 40 mm thick porous panel and a 8 mm acoustic carpet.

In Section 2 of this paper, the measurements of the two materials from two different methods is described and the results are discussed. In Section 3, impedance models are derived and fitted to the measured data to yield broadband impedance results. Finally, in Section 4, the reflection coefficients from the models are approximated as discrete sums of infinite impulse response (IIR) filters to serve as TDBCs. These TDBCs where subsequently used to simulate impulse responses and compare them with measured IRs in (8), of which this paper is a companion.

2 IMPEDANCE MEASUREMENTS

2.1 Methods

Two distinct approaches were used to measure the surface impedances of the acoustic materials: a Kundt's tube method, as laboratory approach of small materials samples, and a pressure-velocity (PU) measurement device, as an in situ approach of the material applied in the room.

2.1.1 Kundt's tube

The Kundt's tube measurements were realised using the so-called transfer function method. The microphones and the speaker used for the measurement are connected to amplifiers which in their turn are connected to a Creative EMU 0202 USB audio device. Impuse responses are acquired from a desktop running Dirac 7841 v6.0 room acoustic software. The working frequency range of the setup used is 100-2500 Hz, the upper value being limited by the relatively large microphone spacing. Further description of the measurement setup can be found in (2).

A 40 mm diameter sample is cut from the material to be placed at one end of the tube. After the sample was placed and the tube carefully sealed, an exponential sweep sine signal is sent through the loudspeaker located at the opposite end of the tube. The impulse response was then captured at 5 different locations within the tube, with one single microphone per measurement in order to avoid microphone calibration errors. The sweep signal used had a duration of 2.73 seconds, and the measurement performed with 8 pre-averages to increase the signal-to-noise ratio. The frequency responses were acquired with a sampling frequency of 192000 Hz and de-convolved into impulse responses by Dirac.

In the post processing part, the impulse responses captured were aligned in time using the measured speaker-to-microphone distances, and the surface impedance was retrieved from the correlated IRs using the transfer functions technique.

2.1.2 In situ PU probe setup

The second setup is an in situ measurement setup making use of a pressure-velocity (PU) sensor, which captures the pressure and particle velocity in one single direction. It is attached to a small spherical loudspeaker, with a speaker-to-sensor distance of 26 cm. The pressure and velocity signal are then connected to a signal conditioner and a front-end. The controls are done from a laptop running the Velo 4.A acquisition software.

The measurement were realized "in situ", directly at the materials mounted in the room. Before measuring, the device was carefully oriented to capture the velocity in the direction of the loudspeaker-probe axis, and a first calibration recording realized with the sensor far from any reflecting plane ("free field measurement"). Subsequently, the device was mounted on a tripod to capture the velocity normal to the sample surface, with a probe-to-sample distance of 10 mm, and the pressure and velocity were captured. The signal used was an internal sweep sine (80 to 12000 Hz) of duration 10 seconds and the measurement was repeated 5 times at different locations on the samples.

The surface impedance was retrieved from the recordings using the so called Mirror-Source method (see in (1)), and a moving average filter was applied on the spectra to reduce the influence from unwanted reflection on the results. The result were then averaged over the various measurement locations. The working frequency range is 300-8000 Hz.

2.2 Results and discussion

As can be seen in Figure 1 (a), the complex surface impedance resulting from the tube and from in situ measurements are in good agreement for the porous panel, particularly above 1 kHz. The wiggles observed in the in situ results below 1 kHz are thought to stem from edge diffraction of the sample measured in situ (see (3)).

However, the surface impedance of the carpet as measured in the tube differs from the in situ measurement, as

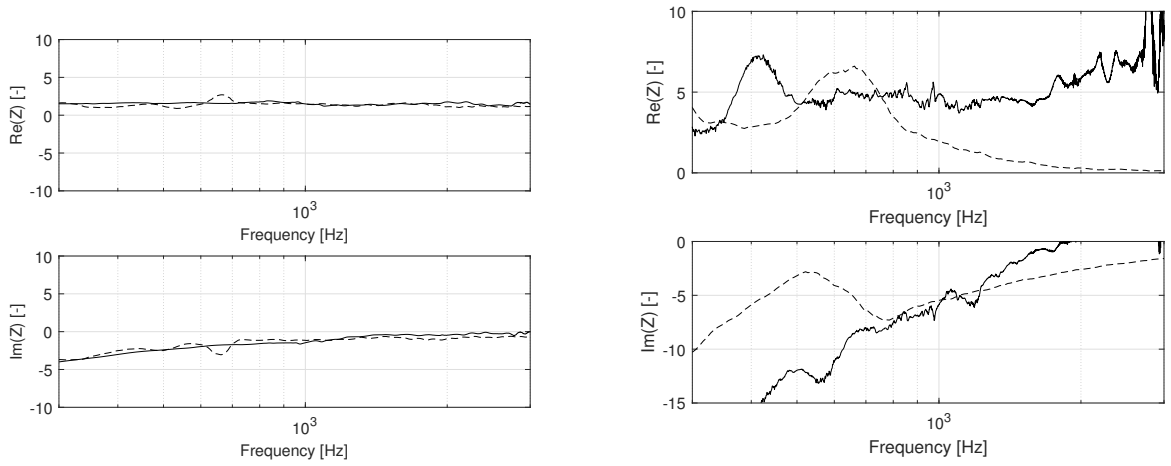

(a) (b)

Figure 1. Comparisons of measured impedances with two different methods. (a): panel, (b): carpet. Plain line: impedance tube, dashed line: PU in situ

seen in Figure 1 (b). Particularly the peak in absorption coefficient, not shown here, was measured by the tube method at a much higher frequency (around 1300 Hz) that what was expected from the commercial data (600 Hz). The reason for this mismatch is likely that the cutting of the sample and/or the mounting in the tube, required for the Kundt's tube measurement, modifies the acoustical properties of the carpet. In the room, carpet tiles of 0.96x0.96 m tiles were measured, while it was cut into a 40 mm diameter disk to fit in the tube. As the surface impedance data needed should be close enough to the one of a sample of infinite dimensions, it seems that the results from the tube yielding irrelevant data.

It appears from the measurement campaign that both measurement methods have drawbacks in capturing acoustical properties of surfaces: The accuracy of the PU-based in situ technique relies much more on factors difficult to control: measurement environment, reflectiveness of the sample under consideration, etc. Whereas the Kundt's tube method allows to measure the lower frequency range more accurately, it also can suffer from the cutting of the sample and the mounting in the tube, that can result in a deterioration of the acoustical properties, as it seems to be the case for the carpet measured here.

3 Model fitting

In order to obtain full-range impedance data of the two materials, broadband impedance models were fitted to the measurement results. This section describes the impedance models used and presents the full-range impedance data obtained after fitting.

3.1 Impedance models

3.1.1 Wall panel

The results from the measurements of the porous panel is compared to the impedance model by Miki for porous media, described in (4). This model takes in account two parameters: the air flow resistivity σ and The thickness of the sample d. In this model the normalized characteristic impedance Z_c and the propagation constant γ of the medium are calculated by empirical laws, that will not be described here for sake of brevity.

3.1.2 Carpet

A 5-parameters model for the carpet has been developed for the resonant carpet. This model assumes that the carpet impedance is a combination of two impedance types (5):

- a porous material impedance, fitted with the aforementioned Miki's model. The fitted impedance is referred to as Z_{porous},
- a ideal membrane resonator impedance. The equivalent resonator is described with: the thickness of the backing air layer d_{res}, the mass per unit area of membrane m, and the damping factor r. The complex surface impedance of the resonator is calculated as

$$Z_{resonator}(f) = \frac{r}{\rho c} + \frac{j}{\rho c}\left(2\pi f m - \rho c \cot\left(\frac{2\pi f}{c} d_{res}\right)\right). \tag{1}$$

The surface impedance of the carpet is then modelled as the parallel circuit equivalent of the two impedances:

$$Z_{carpet} = \frac{Z_{resonator} Z_{porous}}{Z_{resonator} + Z_{porous}}. \tag{2}$$

3.2 Results and Discussion

Fitting of the Miki model to the panel's measurement was realized on the in situ results over the frequency range 300-4000 Hz. The fitted parameters chosen are presented in Table 1 and the comparison of the resulting impedance with the in situ measurements is showed in Figure 2 (a). The model is in agreement with the in situ measurement in the frequency range 300 Hz-4 kHz. The full-range (20 - 20000 Hz) normal incidence absorption coefficient derived from the model is physically admissible over the full range ($0 < \alpha < 1$), as seen in Figure 2 (b).

Parameter [unit]	Fitted value
σ $[Pa \cdot s/m^2]$	63000
d $[mm]$	37

Table 1. Parameters of fitted Miki models

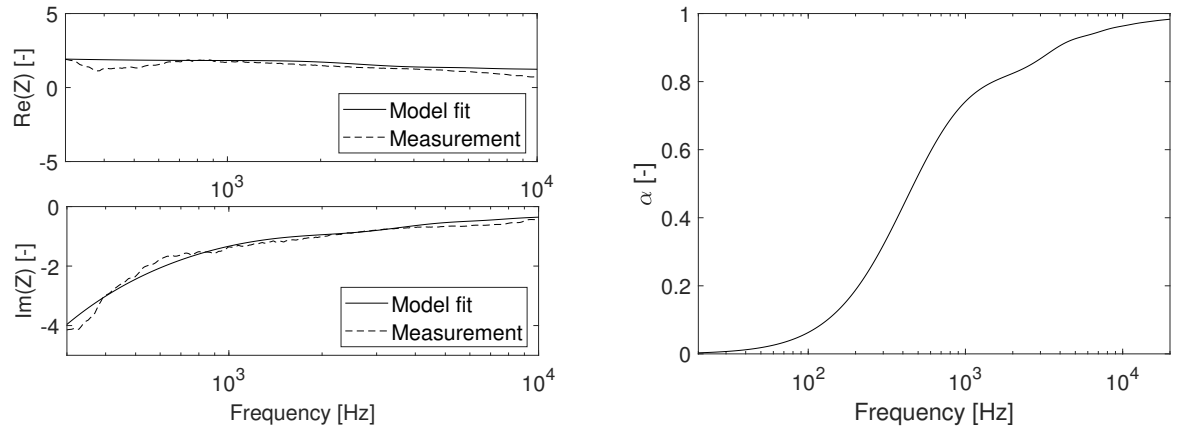

(a) (b)

Figure 2. Porous panel fitted model. (a): Impedance compared to measurements, (b): full range absorption.

Figure 3 (a) shows the fitted model of impedance for the carpet against measurement, as well as the full range, normal incidence absorption coefficient of the model. It can be seen that the agreement is good only above 400 Hz. This could be because the carpet is a more reflective surface than the panel, which decreases the accuracy of the in situ technique at low frequency. Furthermore, the absorption coefficient showed in Figure 3 (b) derived from the model shows to be admissible over the full audible frequency range.

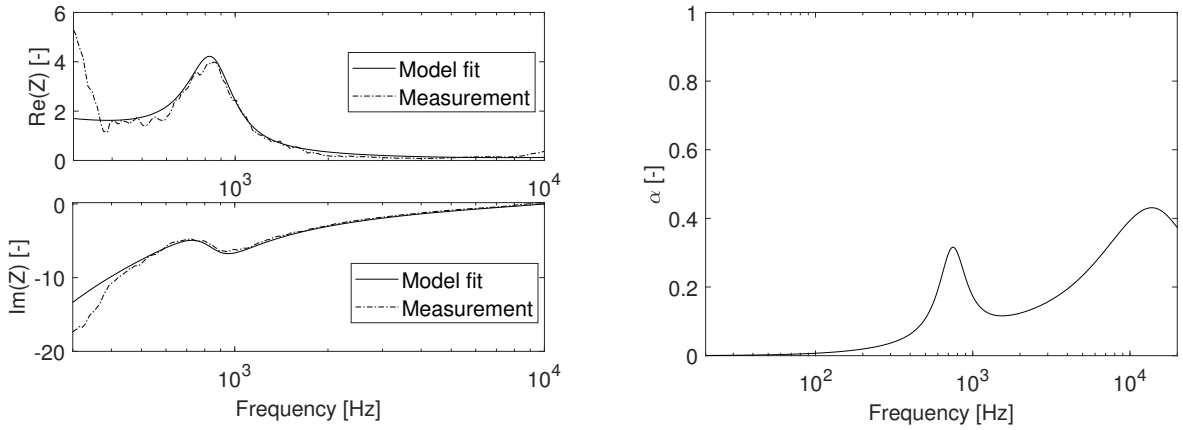

(a) (b)

Figure 3. Carpet fitted model. (a): Impedance compared to measurements, (b): full range absorption.

Parameter	Fitted value
σ $[Pa \cdot s/m^2]$	6500
d $[mm]$	8.5
d_{res} $[mm]$	2.6
m $[g/m^2]$	2300
r $[Pa \cdot s/m]$	5000

Table 2. Parameters of fitted carpet impedance model

4 Derivation of TDBCs

This section describes a method used to derive the TDBC for the two acoustic materials, by approximating the complex reflection coefficient with discrete sums of IIR filters. The approximation covers the range from 20 Hz to 5 kHz.

4.1 TDBC models

To be physically admissible, the frequency-domain representation of the acoustic reflection coefficient must fulfill the conditions of causality, reality and passivity, as described in (6). To obtain such a representation, it is chosen to approximate the spectra of the reflection coefficients (R) with a finite sum of rational functions with single poles, either real valued (λ_k) or pairs of complex conjugates ($\alpha_l \pm i\beta_l$, with α_l and β_l being the the real parts and imaginary parts respectively). This frequency domain approximation of R is written as:

$$R_{approx}(\omega) = \sum_{k=1}^{S} \frac{A_k}{\lambda_k + j\omega} + \sum_{l=1}^{T} \frac{1}{2}\left(\frac{B_l + jC_l}{\alpha_l + j\beta_l + j\omega} + \frac{B_l - jC_l}{\alpha_l - j\beta_l + j\omega} \right), \tag{3}$$

This form fulfills the reality condition ($R_{approx}(-\omega) = \overline{R_{approx}(\omega)}$), and with a proper choice of coefficients, the passivity condition ($|R_{approx}(\omega)| \leq 1$). The causality conditon is met when the poles must have a positive real part, which imposes that $\lambda_k \geq 0$ and $\alpha_l \geq 0$. The time-domain form of the approximated reflection coefficient, r_{TDBC}, to be used as TDBC, can then be analytically computed from the previously obtained coefficient as:

$$r_{TDBC}(t) = \sum_{k=1}^{S} A_k e^{-\lambda_k t} H(t) + \sum_{l=1}^{T} e^{-\alpha_l t} [B_l \cos(\beta_l t) + C_l \sin(\beta_l t)] H(t), \tag{4}$$

where $H(t)$ is the Heaviside step function. This approach to derive TDBC functions for the reflection coefficient was taken from (6), where this method was developed and applied on impedance functions.

4.2 Optimization in the frequency domain

In order to approximate the physical models of reflection coefficients with the appropriate mathematical forms described above, a least-squares minimization in the frequency domain was performed in Matlab. The function to minimize g was chosen to be the norm of the difference between the physical model and the approximation.

$$g(x) = ||R_{approx}(\omega, x) - R_{model}(\omega)||. \tag{5}$$

For this procedure, the reflection coefficients are compared in the frequency range 20 Hz–5 kHz with a frequency resolution of 1 Hz. The TDBC function of the porous panel was chosen to be a sum of real-poles functions only ($T = 0$), and that of the carpet's a sum of complex-poles functions only ($S = 0$). The reason for this is that the absorption mechanism of the porous panel is mostly dissipative and the absorption mechanism of the carpet mostly resonant in the frequency range of interest. The minimization of f yields a set of coefficient x_{min} that allows to construct an approximation of the physical model over the considered frequency range.

4.3 Optimization constraints and parameters

The absolute value of the time-related coefficients of the TDBC functions (in this case: λ_k, α_l and β_l, which are factors of the time variable in equation 3 and 4) should not be too large compared to $1/\Delta t$ (where Δt is the time step of the simulation, estimated to 1e-6s) in order to minimize errors. Similarly to what is done in (7), a maximum value λ_{max} is thus set. This parameter is set relatively to the time resolution intended Δt by using a chosen threshold

$$L = \lambda_{max} \Delta t = 5. \tag{6}$$

The optimization constraints applied to the set of coefficients are finally expressed by the following equations:

$$\begin{aligned} \forall k, \quad & 0 < \lambda_k \Delta t \leq L \\ \forall l, \quad & 0 < \alpha_l \Delta t \leq L \\ \forall l, \quad & |\beta_l| \Delta t \leq L \end{aligned} \tag{7}$$

The number of terms in the sum S (for the panel) and T (for the carpet) is kept as small as possible by performing several tryouts with increasing values, until no improvement of the error is observed. The starting coefficients of the optimizations were chosen randomly in $[0 \quad \lambda_{max}]$ intervals for a set of ten runs, and the result that was minimizing the fitting error was then selected.

4.4 Results

The coefficients and poles of the approximated reflections coefficients for the porous panel and the carpet are displayed in Tables 3 and 4 respectively. The numbers of terms in the resulting IIR sums were $S = 7$ and $T = 8$ for the panel and the carpet respectively.

k	1	2	3	4	5	6	7
A_k	-3.3e4	-1.8e4	1.2e4	1.2e4	1.2e4	1.2e4	1.2e4
λ_k	6.9e3	2.7e3	1.2e4	4.6e3	1.2e4	4.6e3	2.4e3

Table 3. Coefficients of the porous panel's TDBC function.

l	1	2	3	4	5	6	7	8
B_l	-2.5e4	-5.8e4	3.3e4	1.3e4	5.3e5	-1.7e4	-7.2e3	3.1e3
C_l	-1.9e3	-1.4e4	3.7e4	6.3e3	3.2e4	7.8e3	-1.8e4	4.1e4
α_l	2.8e3	5.2e3	1.2e4	2.5e3	9.8e3	1.2e4	9.2e3	5.9e3
β_l	-5.1e3	2.6e3	-4.5e3	5.5e3	4.3e3	-3.8e4	-4.5e4	6.3e3

Table 4. Coefficients for the carpet's TDBC function

As seen in Figure 4 and Table 5, the method used yielded a very close approximation of the reflection coefficients, with a maximum amplitude error smaller than 0.003 and a phase error smaller than 0.006 rad for both materials. Visually, curves from the models and the approximations are nearly indiscernible for both materials, cf. Figure 4. It should also be noted that the approximations functions were also fulfilling the passivity conditions in both case.

Table 5. Maximum fitting error for IIR approximations of R

	Panel	Carpet
$\varepsilon(\lvert R\rvert)$ [-]	0.0020	0.0029
$\varepsilon(\phi(R))$ $[rad]$	0.0044	0.0056

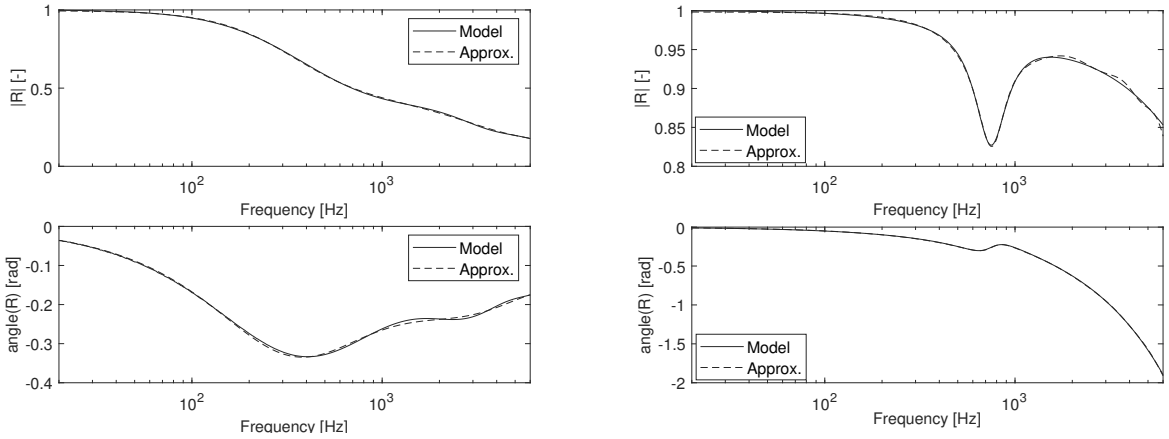

(a) (b)

Figure 4. TDBC approximations of reflection coefficient. (a) panel, (b) carpet.

5 CONCLUSIONS

Physically admissible TDBCs were derived successfully from measurements of a porous panel and a resonant carpet. Surface impedance measurement were carried out, using two different methods, the Kundt's tube ap-

proach and an in situ approach, and the results compared. The results from both approaches were in fairly good agreement for the porouse panel but not for the carpet. Broadband impedance models were then fitted to the measurement results to yield physically admissible, full-range impedance data. The full-range reflection coefficient was subsequently approximated by a sum of IIR filters to provide time-domain boundary conditions.

In the case of the two materials in this study, the fitted impedance models were in fairly good agreement with the measurement data in the 400 Hz-4000 Hz frequency range, while showing physically admissible data in the lower frequency range. The approximation of the resulting full-range data as sum of IIR filters was successful, showing a close agreement between the full-range models and the approximations of the complex reflection coefficient in the 20 Hz-4000 Hz frequency range.

ACKNOWLEDGEMENTS

This work was supported in part by funding from Facebook Technologies, LLC.

REFERENCES

[1] Tijs, E.; Brandao, E.; de Bree, H.E. In situ pu surface impedance measurements for quality control a the end of an assembly line. SAE International, 2009.

[2] Hoekstra, N. Sound absorption of periodically spaced baffles. MSc thesis, Eindhoven University of Technology, 2016.

[3] Brandao, E.; Lenzi, A.; Cordioli, J. Estimation and minimization of errors caused by sample size effect in the measurement of the normal absorption coefficient of a locally reactive surface. Applied Acoustics Vol. 73, 2012

[4] Miki, Y. Acoustical properties of porous materials - modifications of Delany-Bazley models. J. Acoust. Soc. Jpn 11-1, 1990.

[5] Cox, T.J.; D'Antonio, P. Acoustic Diffusers and Absorbers: Theory, Design and Application. CRC Press, 2012.

[6] Reymen, Y.; Baelmans, M.; Desmet, W. Time-domain formulation suited for broadband simulations. 13th AIAA/CEAS Aeroacoustics conference, AIAA paper 2007-3519, 2007

[7] Cotté, B.; Blanc-Benon, P.; Bogey, P; Poisson, F. Time-domain Impedance boundary conditions of outdoor sound propagation. AIAA Journal, Vol. 47, No. 10, October 2009

[8] Georgiou, F.; Briere de La Hosseraye, B.; Hornikx, M.; Robinson, P. Design and simulation of a benchmark room for room acoustic auralizations. Proceedings of International Congress on Acoustics, Aachen, Germany, September 2019.